THE JOURNAL OF BIOLOGICAL CHEMISTRY VOL. 287, NO. 19, pp. 15307–15316, May 4, 2012

The AT-hook Motif-containing Protein AHL22 Regulates Flowering Initiation by Modifying *FLOWERING LOCUS T* Chromatin in *Arabidopsis*[*S]

Received for publication, October 29, 2011, and in revised form, March 20, 2012 Published, JBC Papers in Press, March 22, 2012, DOI 10.1074/jbc.M111.318477

Ju Yun[‡], Youn-Sung Kim[§], Jae-Hoon Jung[‡], Pil Joon Seo[‡], and Chung-Mo Park[‡¶1]

From the [‡]Department of Chemistry, Seoul National University, Seoul 151-742, [‡§]Gendocs, Inc., Daejeon 305-301, and the [¶]Plant Genomics and Breeding Institute, Seoul National University, Seoul 151-742, Korea

Background: AT-hook motif-containing proteins are associated with chromatin modifications.
Results: The *Arabidopsis* AT-hook protein AHL22 regulates H3 acetylation and methylation in *FT* chromatin by binding to an intragenic AT-rich DNA sequence.
Conclusion: AHL22 acts as a chromatin remodeling factor that regulates *FT* expression in flowering induction.
Significance: Learning how the *FT* gene is regulated is critical for understanding gene regulatory mechanisms of flowering.

Coordination of the onset of flowering with developmental status and seasonal cues is critical for reproductive success in plants. Molecular genetic studies on *Arabidopsis* mutants that have alterations in flowering time have identified a wide array of genes that belong to distinct genetic flowering pathways. The flowering time genes are regulated through versatile molecular and biochemical mechanisms, such as controlled RNA metabolism and chromatin modifications. Recent studies have shown that a group of AT-hook DNA-binding motif-containing proteins plays a role in plant developmental processes and stress responses. Here, we demonstrate that the AT-hook protein AHL22 (AT-hook motif nuclear localized 22) regulates flowering time by modifying *FLOWERING LOCUS T* (*FT*) chromatin in *Arabidopsis*. AHL22 binds to a stretch of the AT-rich sequence in the *FT* locus. It interacts with a subset of histone deacetylases. An *Arabidopsis* mutant overexpressing the *AHL22* gene (OE-*AHL22*) exhibited delayed flowering, and *FT* transcription was significantly reduced in the mutant. Consistent with the delayed flowering and *FT* suppression in the OE-*AHL22* mutant, histone 3 (H3) acetylation was reduced and H3 lysine 9 dimethylation was elevated in the *FT* chromatin. We propose that AHL22 acts as a chromatin remodeling factor that modifies the architecture of *FT* chromatin by modulating both H3 acetylation and methylation.

The timing of flowering initiation is regulated through coordinated interactions of developmental programs, such as gibberellic acid, and seasonal cues, including photoperiod, exposure to prolonged low temperature (vernalization), and ambient temperature (1–3). The developmental and environmental signals converge to regulate floral integrators, such as *FT*,[2] *SUPPRESSOR OF OVEREXPRESSION OF CONSTANS 1* (*SOC1*), and *LEAFY* (*LFY*) (2). The *FT* and *SOC1* integrators are also regulated by the floral repressor *FLOWERING LOCUS C* (*FLC*) that incorporates vernalization and autonomous signals into the flowering genetic network (1, 2).

Expression of flowering time genes is modulated through various molecular and biochemical mechanisms in addition to the ordinary gene transcriptional regulation. Examples include controlled RNA metabolism, which is governed primarily by RNA-binding proteins and microRNAs, and epigenetic regulation, which is mediated mainly by histone modifications and DNA methylation (4–7). Several RNA-binding proteins have been shown to regulate RNA processing and selection of polyadenylation sites in their own genes and the *FLC* gene (4, 8). MicroRNAs regulate post-transcriptionally flowering time genes. miR156 suppresses a subset of genes encoding SQUAMOSA PROMOTER BINDING PROTEIN LIKE (SPL) transcription factors that promote flowering (5). MiR172 induces degradation of gene transcripts encoding a small group of APETALA2 (AP2)-like transcription factors that act as floral repressors (5).

Expression of flowering time genes is also regulated by epigenetic mechanisms that include post-translational modifications of histone and nonhistone proteins. Regulation of flowering initiation by histone modifications has been studied extensively in *FLC* chromatin. Molecular characterization of *FLC* repressors and activators in recent years has shown that at

* This work was supported by Leaping Research Program Grant 20110016440 provided by the National Research Foundation of Korea, the Next-Generation BioGreen 21 program (Plant Molecular Breeding Center No. PJ008103) provided by the Rural Development Administration, and Plant Signaling Network Research Center Grant 20110001099, National Research Foundation of Korea Grant 20110027355, the Agricultural R & D Promotion Center Grant 309017-03, and the Korea Ministry for Food, Agriculture, Forestry and Fisheries.

[S] This article contains supplemental Figs. S1–S7 and Table S1.

[1] To whom correspondence should be addressed: Dept. of Chemistry, Seoul National University, 1 Gwanak-Ro, Gwanak-Gu, Seoul 151-742, Korea. Tel.: 82-2-880-6640; Fax: 82-2-886-6697; E-mail: cmpark@snu.ac.kr.

[2] The abbreviations used are: FT, FLOWERING LOCUS T; AHL22, AT-hook motif nuclear localized 22; ATR, AT-rich sequence; BiFC, bimolecular fluorescence complementation; ESC, ESCAROLA; FLC, FLOWERING LOCUS C; FRI, FRIGIDA; GUS, β-glucuronidase; H3, histone 3; H3Ac, H3 acetylation; H3K9me2, H3 dimethylation at Lys-9; H3K27me3, H3 trimethylation at Lys-27; HDAC, histone deacetylase; LFY, LEAFY; MAR, matrix attachment region; MBP, maltose-binding protein; MS, Murashige & Skoog; qRT-PCR, quantitative real-time RT-PCR; SOC1, SUPPRESSOR OF OVEREXPRESSION OF CONSTANS 1; TSA, trichostatin A; YFP, yellow fluorescent protein; BS, binding sequence; LD, long day; CaMV, cauliflower mosaic virus; gFT, genomic FT; cFT cDNA FT; RLN, rosette leaf number.

least three regulatory systems, vernalization, FRIGIDA (FRI), and autonomous pathway components, regulate FLC activity by modifying the *FLC* chromatin. It is known that specific lysine (K) residues in the N-terminal region of H3 are either methylated or acetylated (6). H3 trimethylation at Lys-4 and acetylation are associated with active *FLC* expression. In contrast, H3 deacetylation and methylation at Lys-9 and Lys-27 repress the *FLC* expression (6).

Nuclear matrix is a network of filamentous proteins and somewhat analogous to cellular cytoskeleton (9). Organization of the nuclear matrix is regulated in a temporal and spatial manner during the cell cycle (10, 11). It also contributes to dynamic chromatin reorganization occurring during DNA metabolism and gene expression (9–11). The matrix attachment region (MAR), which is also called the scaffold attachment region, is a stretch of AT-rich DNA sequence (ATR) that guides binding of genomic DNA to the nuclear matrix (10, 11). Therefore, MAR acts as a structural determinant of chromatin organization and recruits multiple MAR-binding factors that facilitate remodeling of the chromatin structure in regulating gene expression (12).

Various MAR-binding factors have been identified in yeast, animals, and plants (11, 12). A major group of the MAR-binding factors possesses a protein motif, called AT-hook that consists of 9–12 residues (13). In animals, many AT-hook proteins have been identified in diverse protein groups, and their roles have been demonstrated in different aspects of gene regulation (13, 14). In plants, a series of AT-hook proteins plays a role in developmental processes, such as flowering transition and stress responses (15–21). One example is the AT-hook motif nuclear localized 22 (AHL22) protein that belongs to the AHL family consisting of 29 members in *Arabidopsis* (22). Overexpression of the *AHL22* gene delays flowering, and *FT* expression is reduced in the transgenic plants (19). In contrast, silencing of four *AHL* genes (*AHL22*, *AHL18*, *AHL27*, and *AHL29*) promotes flowering, suggesting that the *AHL22* gene, and some other *AHL* genes as well, act as a floral repressors, possibly by modulating *FT* expression.

Here, we show that the AHL22 protein binds to an ATR sequence element within the *FT* locus, which has previously been predicted as a intragenic MAR (10), and regulates *FT* expression by recruiting a subset of histone deacetylases, such as HDA1/HDA19, HDA6, and HDA9. H3 acetylation was significantly reduced in the *AHL22*-overexpressing OE-*AHL22* mutant. We also found that H3K9 dimethylation in the *FT* chromatin was elevated in the mutant, suggesting that AHL22 may also interact with histone methyltransferases. Our observations indicate that the *FT* chromatin is coordinately regulated through H3 acetylation and methylation during floral transition.

EXPERIMENTAL PROCEDURES

Plant Materials—Arabidopsis thaliana lines used were in Columbia (Col-0) background. *Arabidopsis* plants were grown in a controlled culture room at 23 °C under long days (LDs, 16-h light/8-h dark). To produce transgenic plants overexpressing *Arabidopsis* genes, the gene sequences were subcloned into the binary pB2GW7 vector under control of the cauliflower mosaic virus (CaMV) 35S-promoter (Invitrogen). The loss-of-function mutants *ahl22-1* and *ahl22-2* (SALK-018866 and SALK-143279, respectively) were isolated from a pool of T-DNA insertion lines deposited in the *Arabidopsis* Biological Resource Center (ABRC, Ohio State University).

Isolation of OE-AHL22 Mutant—The OE-*AHL22* mutant was isolated from an *Arabidopsis* mutant pool that has been produced by randomly integrating the activation tagging vector pSKI015 that contains the CaMV 35S-enhancer element into the genome of Col-0 plants (23). The presence of a single T-DNA insertion event in the OE-*AHL22* mutant was verified by genomic Southern blot analysis using the 35S-enhancer sequence as probe. The flanking genomic sequences of the T-DNA insertion site were determined by a plasmid rescue method (15).

Analysis of Transcript Levels—Transcript levels were examined by either Southern blot hybridization of semi-quantitative RT-PCR products or by quantitative real-time RT-PCR (qRT-PCR). RNA sample preparations, PCR conditions, and data processing have been described previously (23).

qRT-PCR was carried out in 96-well blocks with the Applied Biosystems 7500 Real-time PCR System using the SYBR Green I master mix in a volume of 20 μl. The two-step thermal cycling profile used was denaturation for 15 s at 94 °C and extension for 1 min at 68 °C. The comparative $\Delta\Delta C_T$ method was used to evaluate the relative quantities of each amplified product in the samples. The threshold cycle (C_T) was automatically determined for each reaction by the system set with default parameters. The specificity of amplifications was determined by melt curve analysis of the amplified products using the standard method installed in the system. The *eIF4A* (*eukaryotic initiation factor 4A*) gene (At3g13920) was included in the reactions as internal control for normalizing the variations in the cDNA amounts used. The RT-PCR and qRT-PCR primers used are listed in supplemental Table S1.

Flowering Time Measurements—Plants were grown in soil under LDs until flowering. Flowering times were determined by counting the number of rosette leaves at bolting. Fifteen to 20 plants were counted and averaged for each measurement.

AHL22 Binding to FT DNA—Binding of AHL22 to *FT* DNA was examined using recombinant the maltose-binding protein (MBP)-AHL22 fusion protein essentially as described previously (24) but with some modifications. The recombinant MBP-AHL22 fusion protein was produced in *Escherichia coli* strain BL21-codon Plus (DE3)-RIL (Stratagene, La Jolla, CA). After induction for 5 h at room temperature, *E. coli* cells were harvested and resuspended in lysis buffer A (20 mM Tris-HCl, pH 7.4, 200 mM NaCl, 1 mM EDTA, and 10 mM β-mercaptoethanol) containing protease inhibitor mixture (Sigma) and 1 mM PMSF. The cells were lysed by French press (8500 psi, three times). The cell lysates were sonicated for 30 s twice and centrifuged at 20,000 × *g* for 20 min. The supernatants were stored at −80 °C until use.

For purification of the fusion protein, 1 ml of cell lysates was mixed with amylose resin (New England Biolabs, Ipswich, MA) and incubated at 4 °C for 2 h. The resin was washed 3 times with fresh lysis buffer A. Bound proteins were eluted with 1× SDS-PAGE loading buffer, separated on 10% SDS-PAGE, and trans-

ferred to polyvinylidene fluoride membrane. The air-dried membrane blot was immersed in binding buffer (25 mM HEPES, pH 8.00, 60 mM KCl, 1 mM EDTA, 1 mM DTT, and 6 M guanidine hydrochloride) and gently shaken for 10 min at 4 °C. Renaturation of the bound proteins and MAR-binding assays were carried out as described previously (24).

Chromatin Immunoprecipitation Assays (ChIP)—ChIP assays were performed as described previously (25) using 2-week-old plants grown under LDs on ½ × Murashige & Skoog (MS)-agar plates (hereafter, referred to as MS-agar plates). Briefly, rosette leaves were vacuum-infiltrated with 1% formaldehyde for cross-linking and ground in liquid nitrogen after quenching the cross-linking process. Chromatin preparations were sonicated into 0.5–1-kb fragments. Specific antibodies against MYC (catalog number 05-419), H3Ac (catalog number 06-599), H3K9me2 (catalog number 07-212), and H3K27me3 (catalog number 07-449) (Millipore, Billerica, MA) were added to the chromatin solution, which was precleared with salmon sperm DNA/Protein A-agarose beads. The precipitates were eluted from the beads. Cross-links were reversed, and residual proteins were removed by incubation with proteinase K. DNA was recovered using the QIAquick spin column (Qiagen, Valencia, CA). Quantitative PCR was used to determine the amounts of genomic DNA enriched in the chromatin samples. The primers were designed to amplify DNA fragments of 100–200 bp (supplemental Table S1).

Electrophoretic Mobility Shift Assays (EMSA)—EMSAs were carried out as described previously (25) using recombinant MBP-AHL22 fusion protein. Double-stranded DNA fragments were end-labeled with [γ-^{32}P]ATP using T4 polynucleotide kinase. The radiolabeled DNA fragments were incubated for 30 min at room temperature with 1 μg of the MBP-AHL22 fusion protein in binding buffer (10 mM Tris-HCl, pH 7.6, 50 mM NaCl, 1 mM EDTA, 5 mM DTT, 5% glycerol) supplemented with 100 ng of poly(dI-dC) in the presence or absence of competitor DNA fragments. The reaction mixtures were resolved on 4% nondenaturing polyacrylamide gel. The gel was dried on Whatman 3MM paper and exposed to x-ray films.

Subcellular Localization Assays—A full-size *AHL22* cDNA was fused in-frame to the 3′ end of a green fluorescence protein (GFP)-coding sequence in the p2FGW7 vector (Invitrogen), and the fusion construct was transformed into Col-0 plants. Lateral roots were subject to fluorescence microscopy.

For bimolecular fluorescence complementation (BiFC) assays, a full-size *AHL22* cDNA was fused in-frame to either the 5′ end of a DNA sequence encoding the N-terminal half of EYFP in the pSATN-nEYFP-C1 vector (E3081) or to the 3′ end of a DNA sequence encoding the C-terminal half of EYFP in the pSATN-cEYFP-C1 vector (E3082). The pSAT vectors were kindly provided by Stanton Gelvin (Purdue University). The expression constructs were cotransformed into *Arabidopsis* protoplasts by a polyethylene glycol-calcium transfection method (26). YFP signals were analyzed 14–18 h after transfection by fluorescence microscopy using the Zeiss LSM510 confocal microscope (Carl Zeiss, Yena, Germany).

In Vitro Pulldown Assays—HDAC cDNAs were amplified by RT-PCR and subcloned into the pGBKT7 vector, which contains the SP6 RNA polymerase promoter upstream of the multiple cloning sequence. [^{35}S]-Labeled HDAC proteins were prepared by *in vitro* transcription/translation using the TNT SP6 wheat germ extract-coupled system (Promega, Madison, WI). The *MBP-mAHL22* gene fusion was subcloned into the pMAL-c2X *E. coli* expression vector, and recombinant MBP-mAHL22 protein was prepared as described with the recombinant MBP-AHL22 protein above. *In vitro* pulldown assays were carried out as described previously (27) using 5 μl of ^{35}S-labeled HDAC polypeptides and 5 μg of MBP alone or MBP fusion proteins.

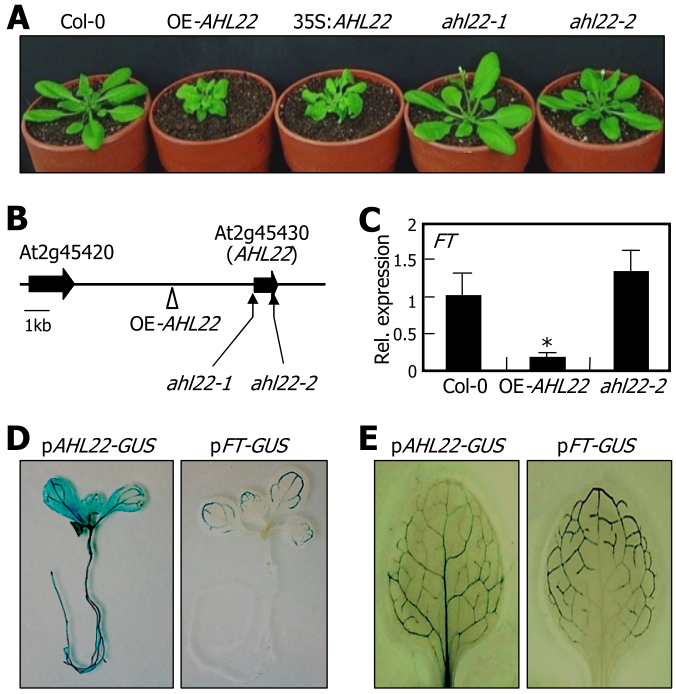

FIGURE 1. **Phenotypic and molecular characterization of OE-*AHL22* and *ahl22* mutants.** *A*, phenotypic comparison. Plants were grown in soil for 4 weeks under LDs before taking photographs. The *AHL22* gene was overexpressed driven by the CaMV 35S-promoter in Col-0 plants, resulting in 35S:*AHL22* transgenic plants. *B*, mapping of the T-DNA insertion events. The *AHL22* gene does not have introns. *C*, *FT* transcript levels. Transcript levels were determined by qRT-PCR. Biological triplicates were averaged and statistically treated using a Student's *t* test (*, $p < 0.01$). *Bars* indicate S.E. of the mean. *D* and *E*, expression domains of *AHL22* and *FT* genes. Whole-mount staining of 8-day-old seedlings (*D*) and staining of the first rosette leaves of 12-day-old seedlings (*E*) were displayed.

Histochemical Staining—A promoter region consisting of a ~2-kbp sequence upstream of the transcription start site of the *AHL22* gene was transcriptionally fused to a β-glucuronidase (GUS)-coding sequence, and the p*AHL22-GUS* fusion was transformed into Col-0 plants. The p*FT-GUS* construct has been described previously (28). Plant sample processing and histochemical detection of GUS activities were carried out as described previously (25).

RESULTS

Pleiotropic Phenotypes of OE-AHL22 Mutant—The *AHL22*-overexpressing OE-*AHL22* mutant exhibited delayed flowering with small, curled rosette leaves (Fig. 1*A* and supplemental Fig. S1*A*). It was also featured by having short siliques and altered floral structure (supplemental Fig. S1, *B* and *C*). We mapped the site of T-DNA insertion by a plasmid rescue method (15). It was found that the T-DNA element was inserted adjacent to the

At2g45430 locus in the mutant (Fig. 1*B*). Genomic Southern blot hybridization confirmed that there was a single T-DNA insertion event in the mutant (supplemental Fig. S2*A*). Gene expression assays showed that the *At2g45430* gene was activated significantly in the mutant (supplemental Fig. S2*B*), suggesting that activation of the *At2g45430* gene correlates with the OE-*AHL22* phenotypes. To examine the co-relationship, the *At2g45430* gene was overexpressed driven by the CaMV 35S-promoter in Col-0 plants. The resulting 35S:*AHL22* transgenic plants recapitulated the OE-*AHL22* phenotypes (Fig. 1*A*), indicating that the *At2g45430* activation underlies the OE-*AHL22* phenotypes. The *At2g45430* gene has previously been named *AT-hook motif nuclear localized 22* (*AHL22*) (19, 22).

Two *AHL22*-deficient mutants, *ahl22-1* and *ahl22-2*, were isolated from the T-DNA insertion pool deposited in the ABRC. The knock-out mutants did not show discernible phenotypes (Fig. 1*A*), possibly because of extensive functional redundancy between *AHL22* and other *AHL* genes (19).

The most prominent phenotype of the OE-*AHL22* mutant was late flowering, as has been observed in *Arabidopsis* mutant overexpressing *ESCAROLA* (*ESC*)/*ORESARA7* (*ORE7*)/*AHL27* gene (15, 17). The early-flowering phenotype of multiple *ahl* mutants also supports the role of the *AHL22* gene and probably other *AHL* genes in flowering time control (19). Expression analysis of flowering time genes showed that the *FT* gene (At1g65480) is significantly suppressed in the OE-*AHL22* mutant (Fig. 1*C* and supplemental Fig. S3*A*). *LFY* and *AP1* genes, which act downstream of the *FT* gene (1, 3), were also suppressed in the mutant. In contrast, expression of the *FT* gene was slightly but reproducibly elevated in the *ahl22* mutants (Fig. 1*C*), suggesting that the late-flowering phenotype of the OE-*AHL22* mutant is at least in part caused by *FT* suppression.

To investigate the potential linkage between the late-flowering phenotype of the OE-*AHL22* mutant and *FT* gene, we compared the spatial expression patterns of the *FT* and *AHL22* genes. The p*AHL22-GUS* construct, in which a promoter region consisting of ~2-kb upstream of the transcription start site of the *AHL22* gene was fused transcriptionally to the GUS-coding sequence, was transformed into Col-0 plants. The p*FT-GUS* fusion has been constructed in a similar manner (28). Histochemical assays revealed that in 8-day-old seedlings, whereas GUS activity was detected broadly in the hypocotyls, roots, and vascular bundles of the leaves in the p*AHL22-GUS* transgenic plants, it was detected primarily in the vascular bundles of the leaves in the p*FT-GUS* transgenic plants (Fig. 1*D*). Close examination of GUS distribution patterns in the leaves of 12-day-old seedlings revealed that GUS activity was detected in the vascular bundles of the basal leaf area in the p*AHL22-GUS* transgenic plants (Fig. 1*E*). In contrast, it was detected in the vascular bundles of the distal leaf area in the p*FT-GUS* transgenic plants, as has been observed (28).

The *AHL22* gene was highly expressed in earlier growth stages, but its expression decreased drastically during the 2–3 week period after germination (supplemental Fig. S3*B*), when *Arabidopsis* plants experience a transition from the juvenile to adult vegetative growth stages (1). In contrast, the *FT* gene exhibited a reversed expression kinetics. Together with *FT* suppression in the OE-*AHL22* mutant, the opposite spatial and temporal expression patterns of the *AHL22* and *FT* genes further support the notion that *FT* suppression is related with the *AHL22*-mediated late flowering.

Binding of AHL22 to FT DNA—AHL proteins possess MAR-binding activity (20, 22). Intragenic MARs are intimately associated with gene regulation (11). We therefore hypothesized that AHL22 might bind to intragenic MARs in the *FT* locus.

In silico mapping of the *Arabidopsis* genome sequence revealed that an ATR sequence element consisting of ~620 nucleotides, which covers parts of introns 1 and 2 and exon 2 of the *FT* gene (Fig. 2*A*), has previously been identified as a putative intragenic MAR (10). An ATR sequence was also predicted in the *AP1* locus (supplemental Fig. S4*A*).

We decided to examine whether AHL22 binds to the ATR sequence in the *FT* locus. Recombinant AHL22 protein was prepared as a MBP-AHL22 fusion in *E. coli* cells. The *FT*-ATR fragment was prepared by genomic PCR and end-labeled with [γ-^{32}P]ATP. Southwestern analysis showed that AHL22 indeed binds to the *FT*-ATR (Fig. 2*B*). AHL22 also bound to the intragenic ATR sequence in the *AP1* locus and the intergenic ATR sequence in the *LFY* locus (supplemental Fig. S4*B*).

The homeobox motif-containing ATHB2 transcription factor, which does not have the AT-hook (29), also bound to the *FT*-ATR. However, the ATHB2-binding DNA fragment, which is a distinct 9-bp dyad-symmetric sequence (CAAT(G/C)ATTG) (30), specifically bound only to ATHB2, but not to AHL22, suggesting that multiple regulatory factors binds to the *FT*-ATR. Sequence comparison identified a putative AT-hook-like sequence in the ATHB2 protein (Fig. 2*C*, *upper panel*). We did not examine whether the sequence motif is responsible for the binding of ATHB2 to the *FT*-ATR. Notably, the *Arabidopsis* high mobility group A protein (At1g14900), which has four AT-hook motifs in the C-terminal region, did not bind to the *FT*-MAR (supplemental Fig. S5), showing that not all AT-hook proteins bind to the *FT*-MAR.

To further examine the AHL22 binding to the *FT*-ATR, a mutated AHL22 protein (mAHL22) was synthesized by mutating the core RGRP sequence to RGAA within the AT-hook motif. The mAHL22 protein did not bind to the *FT*-ATR (Fig. 2*C*, *lower panel*), indicating that the interaction is mediated by the AT-hook, as has been shown with AHL1 (22). Although ATHB2 bound to the *FT*-ATR, additional control transcription factors, such as NTM1 and its activated form ΔC that contain the NAC DNA-binding domain (23), did not exhibit any detectable affinity for the *FT*-ATR, further supporting that AHL22 binding to the *FT*-ATR is specific.

We next examined whether AHL22 binds to the *FT*-ATR *in vivo*, ChIP assays were carried out using 35S:*MYC-AHL22* transgenic plants that overexpress the *MYC-AHL22* gene fusion, in which a MYC-coding sequence was fused in-frame to the 5′ end of the *AHL22* gene. Chromatin preparations extracted from the transgenic seedlings were probed with an anti-MYC antibody. Primer sets were designed so that PCR products of ~200 bp, such as M1, M2, and M3 that cover different regions of the *FT*-ATR (Fig. 2*A*), were synthesized. P1 is a control DNA sequence region that covers the 5′ untranslated

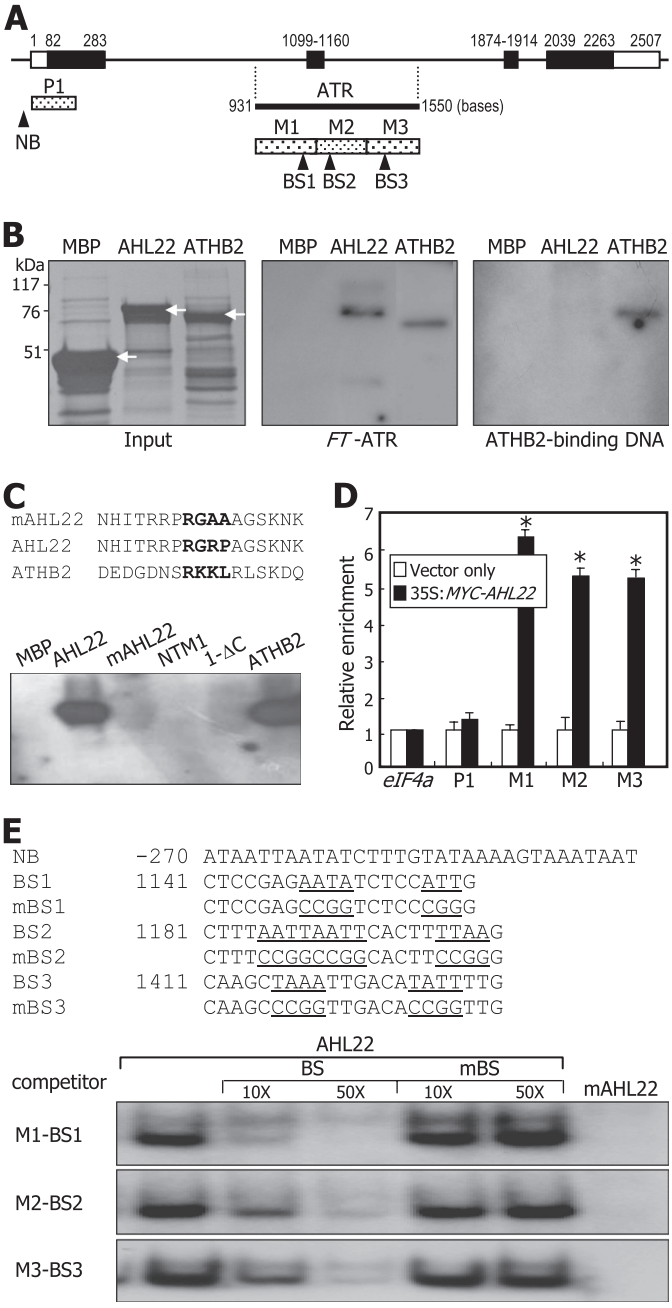

FIGURE 2. **Binding of AHL22 to *FT*-ATR.** *A*, location of ATR in *FT* locus. *Black bars* indicate exons, and *white bars* indicate untranslated regions. The *FT*-ATR was dissected into 3 sequence regions, M1 to M3. *P1* is a control DNA fragment. Putative BSs of AHL22 were selected according to the rule proposed previously (40). *NB*, nonbinding sequence. *B*, AHL22 binding to *FT*-ATR. Recombinant AHL22 and ATHB2 proteins were prepared as MBP fusions in *E. coli* cells (*left panel*, *white arrows*). The same amounts of proteins shown on the protein gel and ^{32}P-labeled DNA fragments were used in the *in vitro* binding assays (*middle panel*). The ATHB2-binding sequence was also assayed (*right panel*). *C*, effects of core sequence mutations on AHL22 binding to *FT*-ATR. The core sequence of the AT-hook motif (RGRP) was mutated to RGAA, resulting in mAHL22 (*upper panel*). NTM1 and ATHB2 transcription factors were included as controls in the assays (*lower panel*). *D*, ChIP assays on AHL22 binding to *FT*-ATR. The 35S:*MYC-AHL22* transgenic plants grown on MS-agar plates for 2 weeks were used. Primer pairs specific to M1, M2, and M3 sequences were used. Three measurements were averaged and statistically treated (*t* test, $^{*}p < 0.01$). *Bars* indicate mean ± S.E. *E*, EMSA on AHL22 binding to *FT*-ATR. The BS sequences were mutated to verify specific binding, resulting in mutated BS (*mBS*) sequences (*upper panel*). Increasing amounts of unlabeled BS or mutated BS oligonucleotides were added to the assay mixtures (*lower panel*).

region and part of exon 1, to which the *FT* repressor TEMPRANILLO 1 binds (31). The assays using the primer sets covering the M1, M2, and M3 regions showed clear enrichment of the *FT*-ATR sequence, whereas those covering the P1 region did not show any enrichment of the *FT*-ATR sequence (Fig. 2*D*). In addition, AHL22 binding to the M1 and M3 regions was further elevated in 35-day-old plants compared with that in 10-day-old plants (supplemental Fig. S6), which is certainly due to the developmental stage-dependent activation of *FT* chromatin (1). These observations demonstrate that AHL22 binding to the *FT*-ATR occurs *in vivo*.

We also carried out EMSA using DNA sequences bearing AAT, ATT, TAA, and TTA within the *FT*-ATR as probes (Fig. 2*E*, *upper panel*). The DNA fragments of ~20 nucleotides containing the consensus motifs were end-labeled, and their binding to recombinant MBP-AHL22 fusion protein was assayed. It was found that AHL22 bound strongly to the binding sequences (BSs) that are homologous to the *FT*-ATR (Fig. 2*E*, *lower panel*). In addition, the AHL22 binding was significantly reduced in the presence of excess unlabeled BS fragments but only slightly reduced in the presence of mutated DNA fragments (mBSs), supporting the specific binding of AHL22 to the BS sequences. In contrast, we did not detect any detectable binding of mAHL22 to the BS sequences.

Effects of AT-hook Mutation on AHL22 Function in Flowering—We next examined whether AHL22 binding to the *FT*-ATR is physiologically important in flowering. To examine this, the *mAHL22* gene was overexpressed in *Arabidopsis*. Unlike the late-flowering 35S:*AHL22* transgenic plants, the 35S:*mAHL22* transgenic plant did not exhibit late flowering (Fig. 3*A*). qRT-PCR assays revealed that the *mAHL22* transcript level in the 35S:*mAHL22* transgenic plant was similar to that in the OE-*AHL22* mutant (Fig. 3*B*, *left panel*). In contrast, the *FT* transcript level was not reduced in the 35S:*mAHL22* transgenic plant, which was in contrast to the significant suppression of the *FT* gene in the OE-*AHL22* mutant (Fig. 3*B*, *right panel*). These observations indicate that AHL22 binding to the *FT*-ATR is linked with the AHL22-mediated delaying flowering.

Based on the specific binding of AHL22 to the *FT*-ATR, it was predicted that AHL22 would be localized in the nucleus. We examined the subcellular localization of AHL22 using transgenic plants overexpressing a GFP-AHL22 fusion, in which a GFP-coding sequence was fused in-frame to the 5′ end of the *AHL22* gene. The assays showed that AHL22 is localized exclusively in the nucleus (Fig. 3*C*). The mAHL22 protein was also localized in the nucleus, indicating that the AT-hook motif is not essential for the nuclear localization of AHL22.

The subcellular distribution of the AHL22 and mAHL22 proteins was further examined by transiently expressing the GFP-AHL22 and GFP-mAHL22 fusions in *Arabidopsis* protoplasts. Both the AHL22 and mAHL22 proteins were localized exclusively in the nucleus (Fig. 3*D*), demonstrating that the AHL22 protein is localized in the nucleus, where it binds to the *FT*-ATR.

AHL22 Suppression of FT in Flowering—Our data showed that AHL22 suppresses *FT* expression by binding directly to the *FT*-ATR. Therefore, a question was whether the AHL22 suppression of *FT* is physiologically important in flowering.

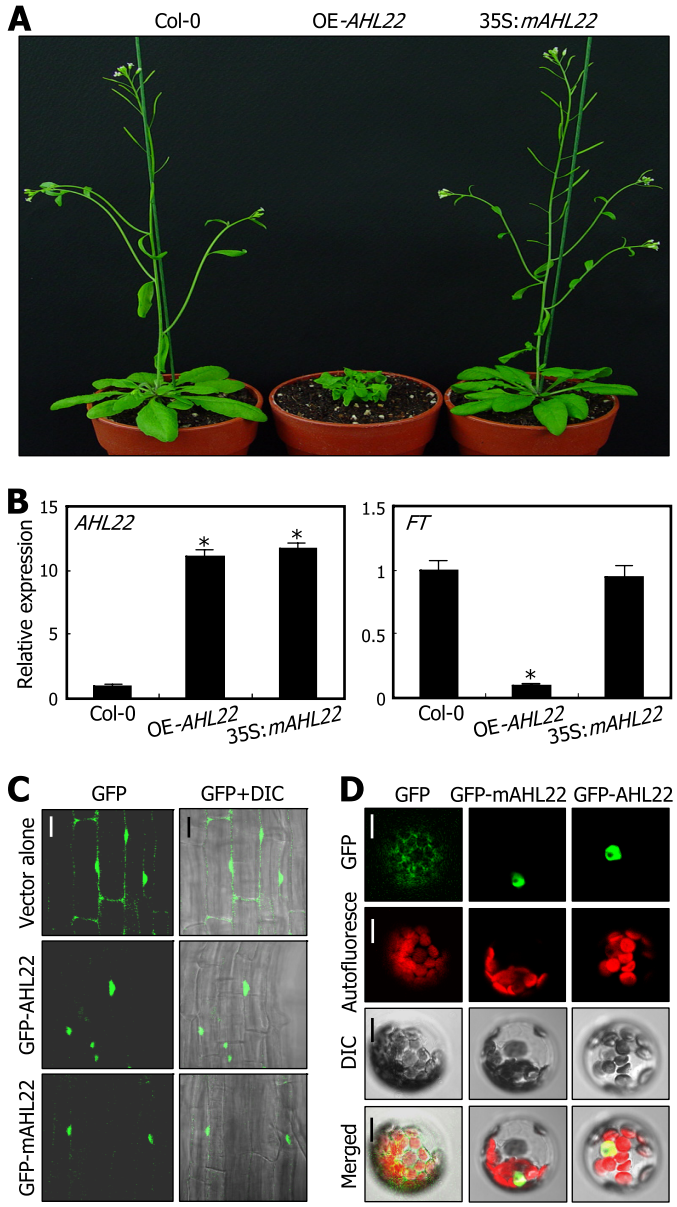

FIGURE 3. **Effects of *AHL22* mutation on *FT* expression and flowering.** *A*, flowering phenotypes of 35S:*mAHL22* transgenic plants. *B*, relative transcript levels of *FT* and *AHL22* genes. Two-week-old whole plants grown on MS-agar plates were used for extraction of total RNA. Transcript levels were determined by qRT-PCR. Biological triplicates were averaged and statistically treated (*t* test, *, $p < 0.01$). *Bars* indicate mean ± S.E. *C* and *D*, subcellular localization of AHL22 proteins. The *GFP-AHL22* and *GFP-mAHL22* gene fusions were either transformed into Col-0 plants (*C*) or transiently expressed in *Arabidopsis* protoplasts (*D*). In *C*, root samples were visualized by differential interference contrast microscopy (*DIC*) and fluorescence microscopy. *Scale bar*, 40 μm. In *D*, *Arabidopsis* protoplasts were examined by confocal microscopy. *Scale bar*, 10 μm.

To address the question, we produced two independent transgenic plants: one overexpressing the genomic *FT* gene sequence (*gFT*) and the other overexpressing *FT* cDNA (*cFT*). The *gFT* gene consisting of 2180 bp included four exons and three introns (Fig. 4*A*). It also included the *FT*-ATR. In contrast, the *cFT* gene consisting of 528 bp lacks intact *FT*-ATR, and thus AHL22 is unable to bind to the *FT* cDNA. The 35S:*gFT* and 35S:*cFT* transgenic plants were also genetically crossed with the late-flowering OE-*AHL22* mutant, resulting in 35S:*gFT* OE-*AHL22* and 35S:*cFT* OE-*AHL22* plants.

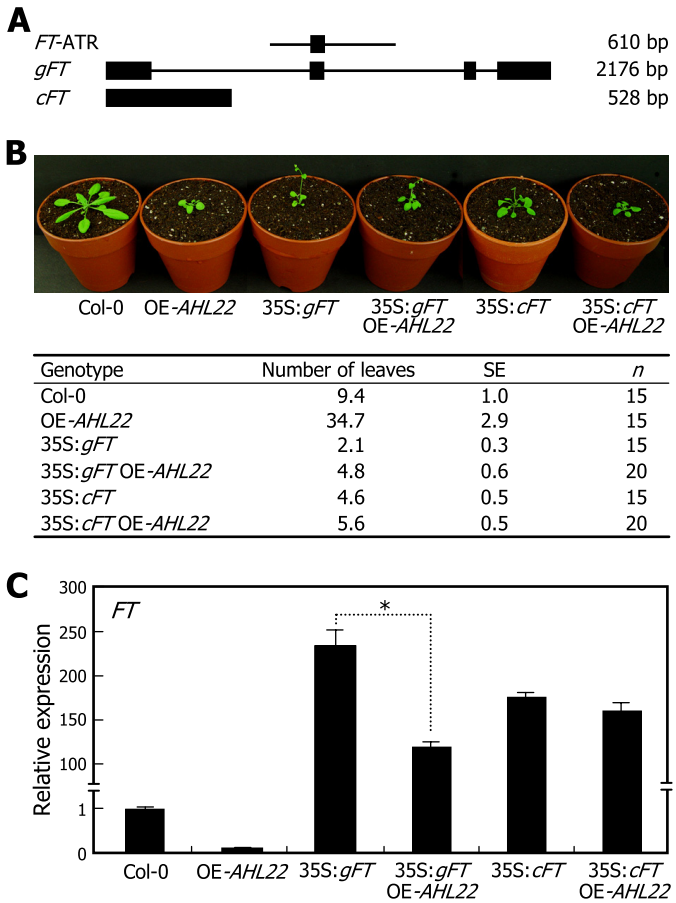

Genotype	Number of leaves	SE	*n*
Col-0	9.4	1.0	15
OE-*AHL22*	34.7	2.9	15
35S:*gFT*	2.1	0.3	15
35S:*gFT* OE-*AHL22*	4.8	0.6	20
35S:*cFT*	4.6	0.5	15
35S:*cFT* OE-*AHL22*	5.6	0.5	20

FIGURE 4. **AHL22 suppression of *FT* gene in flowering.** *A*, *FT* gene constructs used. *Black boxes* indicate exons. *B*, flowering phenotypes of transgenic plants overexpressing either *gFT* or *cFT* sequences. Four-week-old plants grown in soil under LDs were photographed (*upper panel*). Flowering times were measured by counting rosette leaf numbers at bolting (*lower panel*). Fifteen to 20 plants were counted and averaged for each plant genotype. Values are mean ± S.E. *C*, *FT* transcript levels. Whole plants grown on MS-agar plates for 10 days under LDs were used for extraction of total RNA. Transcript levels were determined by qRT-PCR. Biological triplicates were averaged and statistically treated (*t* test, *, $p < 0.01$). *Bars* indicate mean ± S.E.

Both the 35S:*gFT* and 35S:*cFT* transgenic plants flowered very early at rosette leaf numbers (RLN) of 2.1 ± 0.3 and 4.6 ± 0.5, respectively (Fig. 4*B*). The *FT* transcript levels were accordingly elevated drastically in the transgenic plants (Fig. 4*C*). The 35S:*gFT* OE-*AHL22* and 35S:*cFT* OE-*AHL22* plants also exhibited early flowering (Fig. 4*B*). However, counting of the RLN revealed that the early-flowering phenotype of the 35S:*gFT* transgenic plants was detectably repressed in the 35S:*gFT* OE-*AHL22* plants, which flowered at a RLN of 4.8 ± 0.6. In contrast, the early-flowering phenotype of the 35S:*cFT* transgenic plants were suppressed only slightly in the 35S:*cFT* OE-*AHL22* transgenic plants, which flowered at a RLN of 5.6 ± 0.5.

Consistent with the changes in flowering times, the *FT* transcript level was detectably reduced in the 35S:*gFT* OE-*AHL22* plants compared with that in the 35S:*gFT* transgenic plants (Fig. 4*C*). In contrast, the *FT* transcript level in the 35S:*cFT* OE-*AHL22* plants was largely unchanged compared with that in the 35S:*cFT* transgenic plants, which is certainly because the *FT* cDNA is not targeted by AHL22. These observations demonstrate that AHL22 regulates flowering time by modulating *FT* expression.

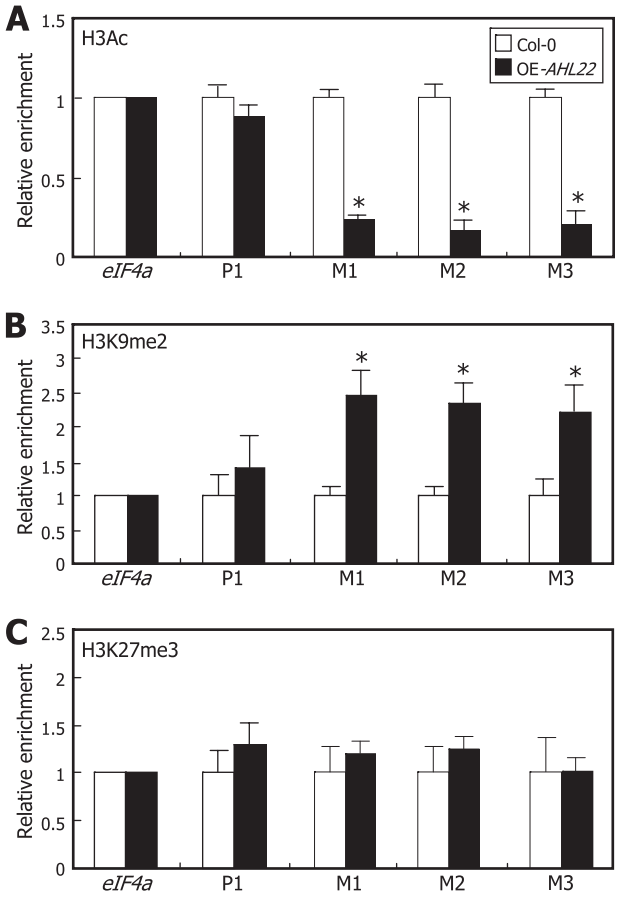

FIGURE 5. **Modifications of *FT* chromatin by AHL22.** Relative levels of H3 modifications in *FT* chromatin were examined by ChIP assays using an anti-H3Ac (*A*), -H3K9me2 (*B*), or -H3K27me3 (*C*) antibody. PCR primer pairs specific to M1, M2, and M3 sequences, as shown in Fig. 2*A*, were used. Plants grown on MS-agar plants for 12 days under LDs were used for chromatin preparations. Three measurements were averaged and statistically treated (*t* test, *, $p < 0.01$). *Bars* indicate mean ± S.E.

AHL22 Regulation of H3 Acetylation and Methylation in FT Chromatin—Recent studies have shown that some AT-hook proteins function in chromatin remodeling in both animals and plants (13). MAR-binding factors play a role in gene regulation by mediating chromatin modifications (11, 14). Our data showed that AHL22 interacts with the *FT*-ATR, which has been suggested to act as an intragenic MAR (10). We therefore examined whether AHL22 repression of *FT* transcription is mediated by histone modifications.

We carried out ChIP assays on the *FT* chromatin using the primer sets used in the ChIP assays on AHL22 binding to *FT*-ATR (Fig. 2*D*). The ChIP assays revealed that H3 acetylation (H3Ac), which is a mark for active gene expression (32), was reduced ~70% in the *FT*-ATR in the OE-*AHL22* mutant compared with that in Col-0 plants (Fig. 5*A*). In contrast, H3 dimethylation at Lys-9 (H3K9me2), a repressive mark for gene expression (33), increased ~2-fold in the mutant (Fig. 5*B*). These observations indicate that AHL22 modulates *FT* chromatin within the *FT*-ATR by modulating H3 acetylation and Lys-9 dimethylation. In contrast, H3 trimethylation at Lys-27 (H3K27me3), which is another repressive mark for gene expression (34), was not changed to a discernible level in the mutant (Fig. 5*C*), suggesting that H3K27me3 is not involved in the AHL22-mediated modifications of the *FT* chromatin.

Interactions of AHL22 with HDACs—Histone deacetylases (HDACs) are a group of enzymes that remove acetyl groups from acetylated Lys residues of histone proteins (35). We found that H3 acetylation is reduced in the *FT* chromatin of the OE-*AHL22* mutant. We therefore asked whether the AHL22-mediated modifications of *FT* chromatin are related to HDACs.

We first carried out *in vitro* pulldown assays using recombinant MBP-AHL22 fusion protein and *in vitro* translated HDAC polypeptides to examine whether AHL22 interacts with HDAC enzymes. It was found that AHL22 strongly interacted with HDA1/HDA19, HDA6, and HDA9 (Fig. 6*A*), which are involved in flowering timing and floral architecture (35). The three HDAC proteins did not bind to MBP alone, supporting the specific interaction between the HDAC enzymes and AHL22 protein.

We also carried out BiFC assays to further examine the AHL22-HDAC interactions. The nYFP- and cYFP-coding sequences were fused in-frame to the 5′ and 3′ ends of the *AHL22* and *HDAC* gene sequences, and the fusion constructs were coexpressed transiently in *Arabidopsis* protoplasts. Strong reconstituted YFP signals were detected in the nuclei of cells coexpressing the AHL22-nYFP and HDAC-cYFP fusions and the AHL22-cYFP and HDAC-nYFP fusions (Fig. 6*B*), confirming that AHL22 interacts with the HDAC enzymes in the nucleus.

Dynamic dimer formation regulates the binding specificity and affinity of transcription regulators to their target DNA or interacting partners (36). We therefore examined whether AHL22 forms homodimers by *in vitro* pulldown assays using recombinant MBP-AHL22 proteins and [^{35}S]methionine-labeled AHL22 polypeptides. We found that the two AHL22 forms interact with each other (supplemental Fig. S7*A*). In addition, BiFC assays in *Arabidopsis* protoplasts showed that the two AHL22 forms interact with each other *in vivo* (supplemental Fig. S7*B*). Notably, the mAHL22 protein also interacts with AHL22 in both *in vitro* pulldown assays and BiFC assays (supplemental Fig. S7, *A* and *B*), indicating that the AT-hook motif is not required for the interactions. These observations support that the AHL22 proteins form multimers, probably homodimers.

We next examined whether HDAC activity is important for *FT* regulation by employing trichostatin A (TSA) that selectively inhibits class I and II mammalian HDAC enzymes (35). *Arabidopsis* plants were grown for 10 days on MS-agar plates containing 0.5 μM TSA, and *FT* transcript levels were examined. The *FT* transcript level was elevated at least 7-fold in the TSA-treated OE-*AHL22* mutant (Fig. 6*C*). In contrast, the *AHL22* transcription was not affected by TSA under identical conditions, indicating that HDACs participate in the AHL22-mediated suppression of *FT* transcription.

Altogether, our data demonstrate that the AHL22 protein suppresses *FT* transcription by binding to the *FT*-ATR and recruiting a subset of HDAC enzymes. A plausible working scenario is that the AHL22-HDAC complexes deacetylate acetylated histones in the *FT* chromatin (Fig. 6*D*). AHL22 also regulates H3 dimethylation at Lys-9, suggesting that histone

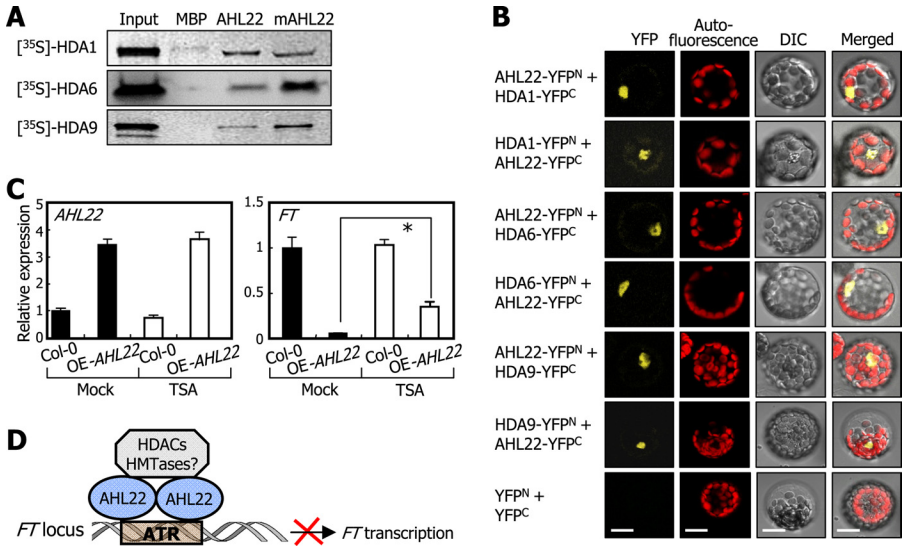

FIGURE 6. **Interaction of AHL22 with HDACs.** *A*, *in vitro* pulldown assays. [^{35}S]-Labeled HDAC polypeptides were prepared by *in vitro* translation. Recombinant MBP-AHL22 and MBP-mAHL22 proteins prepared in *E. coli* cells were used. *Input* represents 5% of the HDAC protein used in each assay. *B*, BiFC assays in *Arabidopsis* protoplasts. The cYFP and nYFP fusions were cotransfected into *Arabidopsis* protoplasts and visualized by differential interference contrast (*DIC*) microscopy and fluorescence microscopy. *Scale bar*, 10 μm. *C*, effects of *TSA* on *FT* expression in OE-*AHL22* mutant. Transcript levels were determined by qRT-PCR. Biological triplicates were averaged and statistically treated using a Student's *t* test (*, $p < 0.01$). *Bars* indicate mean ± S.E. *D*, schematic model of AHL22 function in flowering.

methyltransferases are also involved in the AHL22-mediated modification of the *FT* chromatin.

DISCUSSION

The AHL proteins are characterized by having two conserved structural components: the AT-hook motif that binds to AT-rich stretches of DNA and the plant and prokaryotic conserved domain that mediates nuclear localization (22). Several AHL proteins have been functionally studied in diverse aspects of plant growth and developmental processes and stress responses in *Arabidopsis*. AGF1/AHL25 is critical for the negative feedback regulation of GA3 oxidase gene (16). SOB3/AHL29 and ESC/ORE7/AHL27 are known to regulate hypocotyl growth (18). It also acts as a negative regulator of leaf senescence (17). In addition, GIK/AHL21 plays a role in organ patterning and differentiation (20). Furthermore, it has been reported that AHL22 is involved in flowering induction and hypocotyl elongation (19). Meanwhile, overexpression of the *AHL20* gene suppresses plant innate immune responses (21). AHL15, AHL19, and AHL27 have also been implicated in defense responses (21).

It is notable that AHL1 binds to MARs via the AT-hook motif (22). MARs are specific stretches of DNA sequences that are important for the structural organization of chromatin fibers by anchoring chromatin loops to nuclear matrix (10). A genome-scale study of gene expression patterns in conjunction with screening of potential intragenic MARs has shown that *Arabidopsis* genes possessing intragenic MARs tend to be less expressed irrespective of plant tissues and organs and differentially regulated throughout the plant growth stages (10, 11). It has been known that MARs link AHL proteins with chromatin modifications. For example, ESC/ORE7/AHL27 influences chromatin architecture by modulating the distribution of H2B (17). In addition, AHL21 represses the *AUXIN RESPONSE FACTOR 3* (*ARF3*) gene by inducing H3 dimethylation at Lys-9 in the gene promoter during floral development (20).

In this work, we demonstrated that AHL22 suppresses *FT* expression by binding to the *FT*-ATR and recruiting a subset of HDAC enzymes, HDA1/HDA19, HDA6, and HDA9. The early-flowering phenotype of the 35S:*gFT* transgenic plants was compromised in the OE-*AHL22* background (35S:*gFT* OE-*AHL22*). Consistent with the changes in flowering time, the *FT* transcript level was reduced in the 35S:*gFT* OE-*AHL22* plants compared with that in the 35S:*gFT* transgenic plants. In contrast, the early-flowering phenotype of the 35S:*cFT* transgenic plants was reduced only slightly in the OE-*AHL22* background (35S:*cFT* OE-*AHL22*), which is obviously because the *FT* cDNA does not have intact *FT*-ATR to which AHL22 binds.

More work is required to determine whether AHL22 is a *bona fide* MAR-binding factor and the *FT*-ATR is an intragenic MAR. The *FT*-ATR has been predicted as an intragenic MAR (10). A major group of MAR-binding factors possesses the AT-hook motif (13). AHL1 is associated with the nuclear matrix (22). It is therefore likely that AHL22 acts as a MAR-binding factor in *Arabidopsis*.

Our data strongly support that AHL22 regulates *FT* expression by modulating histone acetylation and methylation through physical interactions with HDACs and presumably methyltransferase enzymes. Whereas the level of H3Ac was reduced, that of H3K9me2 was elevated in the *FT* chromatin of the late-flowering OE-*AHL22* mutant, whereas H3K27 trimethylation may not be involved in *FT* control (Fig. 5). The physiological significance of the AHL22-HDAC interactions in *FT* regulation and thus flowering time control is further supported by the effects of the HDAC inhibitor TSA on *FT* expression in the OE-*AHL22* mutant. However, the role of the AHL22-HDAC interactions in flowering time control likely is more complicated than the proposed working model (Fig. 6*D*). AHL

proteins are functionally redundant, and at least several AHL proteins are apparently involved in flowering time control (18, 19, 21), suggesting that different AHL proteins may interact with different HDAC enzymes. This view entails that various combinations of AHL-HDAC complexes would bind to the *FT*-ATR, depending on developmental and environmental signals.

We observed that *LFY* and *AP1* genes, in addition to *FT*, are also suppressed in the OE-*AHL22* mutant (supplemental Fig. S3*A*). In addition, AHL22 bound to the intragenic and intergenic ATR sequences in the *AP1* and *LFY* loci, respectively. It is therefore likely that the AHL22-HDAC complexes also regulate the chromatin status of *LFY* and *AP1* genes and other flowering time genes in addition to the *FT* gene. This signaling complexity may explain the relatively small changes of *FT* transcript levels and the timing of flowering initiation observed in the 35S:*gFT* OE-*AHL22* plants compared with those in the 35S:*gFT* transgenic plants. Further work is necessary to determine how much the AHL22-HDAC regulation of *FT* chromatin contributes to the role of FT in flowering time control. In addition, the role of endogenous and environmental factors in regulating AHL22 activity should also be investigated.

Coordinated histone modifications mediate epigenetic regulation of gene expression in plants. One of the most extensively studied is epigenetic regulation of the floral repressor *FLC*. It has been known that epigenetic regulation of the *FLC* gene is mediated by complex networks of histone acetylation and methylation events. Activation of the *FLC* expression is achieved through several active chromatin modifications, such as acetylation of core histone tails, H3K4 methylation, and H3K36 dimethylation and trimethylation (6). In contrast, repressive histone modifications, including histone deacetylation, H3K4 demethylation, H3K9 and H3K27 methylation, and histone arginine methylation, repress the *FLC* expression (6).

Histone modifications in *FT* chromatin have recently been studied. Whereas H3K4 trimethylation in the *FT* chromatin is associated with *FT* activation, H3K27 trimethylation is associated with *FT* repression. It has been found that the H3K27 methyltransferase CURLY LEAF (CLF) represses *FT* expression (37). In addition, the chromodomain-containing LIKE HETEROCHROMATIN PROTEIN 1 (LHP1) protein binds to H3K27me3 in the *FT* chromatin and maintains the repressive state of *FT* expression (38). However, there is little known about the role of histone acetylation/deacetylation in the *FT* chromatin. We found that AHL22 binds to an AT-rich DNA sequence in the *FT* locus and reduces H3 acetylation. We also found that H3 dimethylation at Lys-9 is elevated in the *FT* chromatin of the OE-*AHL22* mutant. It seems that the *FT* chromatin is regulated through coordinated actions of histone acetylation and methylation, although not precisely in the way that epigenetic modifications control the *FLC* gene.

HDAC enzymes play a role in global gene repression during developmental processes and stress adaptation responses in plants (35). AHL22 physically interacts with HDA1/HDA19, HDA6, and HDA9, which are homologous to yeast RPD3 (reduced potassium deficiency 3) and belong to the type I HDAC subfamily (35). In *Saccharomyces pombe*, mutations in the subunits of class I HDAC complexes affect H3K9 methylation (39), indicating that Lys-9 deacetylation is a prerequisite for subsequent H3 methylation. We found that H3K9 dimethylation was elevated in the *FT* chromatin of the OE-*AHL22* mutant. Based on the previous and our own data, we believe that AHL22 regulates the *FT* chromatin in a similar manner to the yeast RPD3: H3 deacetylation by HDAC enzymes may precede H3K9 dimethylation to suppress *FT* expression. In this view, it is envisaged that AHL22 may also interact with histone methyltransferases (Fig. 6*D*).

Acknowledgment—We thank the Arabidopsis Biological Resource Center for the SALK T-DNA lines.

REFERENCES

1. Amasino, R. (2010) Seasonal and developmental timing of flowering. *Plant J.* **61,** 1001–1013
2. Simpson, G. G., and Dean, C. (2002) *Arabidopsis*, the Rosetta stone of flowering time? *Science* **296,** 285–289
3. Blázquez, M. A., Ahn, J. H., and Weigel, D. (2003) A thermosensory pathway controlling flowering time in *Arabidopsis thaliana*. *Nat. Genet.* **33,** 168–171
4. Simpson, G. G. (2004) The autonomous pathway. Epigenetic and post-transcriptional gene regulation in the control of *Arabidopsis* flowering time. *Curr. Opin. Plant Biol.* **7,** 570–574
5. Jones-Rhoades, M. W., Bartel, D. P., and Bartel, B. (2006) MicroRNAS and their regulatory roles in plants. *Annu. Rev. Plant Biol.* **57,** 19–53
6. He, Y. (2009) Control of the transition to flowering by chromatin modifications. *Mol. Plant* **2,** 554–564
7. Yaish, M. W., Colasanti, J., and Rothstein, S. J. (2011) The role of epigenetic processes in controlling flowering time in plants exposed to stress. *J. Exp. Bot.* **62,** 3727–3735
8. Liu, F., Marquardt, S., Lister, C., Swiezewski, S., and Dean, C. (2010) Targeted 3′ processing of antisense transcripts triggers *Arabidopsis* FLC chromatin silencing. *Science* **327,** 94–97
9. Pederson, T. (2000) Half a century of "the nuclear matrix." *Mol. Biol. Cell* **11,** 799–805
10. Rudd, S., Frisch, M., Grote, K., Meyers, B. C., Mayer, K., and Werner, T. (2004) Genome-wide *in silico* mapping of scaffold/matrix attachment regions in *Arabidopsis* suggests correlation of intragenic scaffold/matrix attachment regions with gene expression. *Plant Physiol.* **135,** 715–722
11. Tetko, I. V., Haberer, G., Rudd, S., Meyers, B., Mewes, H. W., and Mayer, K. F. (2006) Spatiotemporal expression control correlates with intragenic scaffold matrix attachment regions (S/MARs) in *Arabidopsis thaliana*. *PLoS Comput. Biol.* **2,** e21
12. Wang, T. Y., Han, Z. M., Chai, Y. R., and Zhang, J. H. (2010) A minireview of MAR-binding proteins. *Mol. Biol. Rep.* **37,** 3553–3560
13. Aravind, L., and Landsman, D. (1998) AT-hook motifs identified in a wide variety of DNA-binding proteins. *Nucleic Acids Res.* **26,** 4413–4421
14. Reeves, R. (2010) Nuclear functions of the HMG proteins. *Biochim. Biophys. Acta* **1799,** 3–14
15. Weigel, D., Ahn, J. H., Blázquez, M. A., Borevitz, J. O., Christensen, S. K., Fankhauser, C., Ferrándiz, C., Kardailsky, I., Malancharuvil, E. J., Neff, M. M., Nguyen, J. T., Sato, S., Wang, Z. Y., Xia, Y., Dixon, R. A., Harrison, M. J., Lamb, C. J., Yanofsky, M. F., and Chory, J. (2000) Activation tagging in *Arabidopsis*. *Plant Physiol.* **122,** 1003–1013
16. Matsushita, A., Furumoto, T., Ishida, S., and Takahashi, Y. (2007) AGF1, an AT-hook protein, is necessary for the negative feedback of AtGA3ox1 encoding GA 3-oxidase. *Plant Physiol.* **143,** 1152–1162
17. Lim, P. O., Kim, Y., Breeze, E., Koo, J. C., Woo H. R., and Ryu J. S. (2007) Overexpression of a chromatin architecture-controlling AT-hook protein extends leaf longevity and increases the post-harvest storage life of plants. *Plant J.* **52,** 1140–1153
18. Street, I. H., Shah, P. K., Smith, A. M., Avery, N., and Neff, M. M. (2008) The AT-hook-containing proteins SOB3/AHL29 and ESC/AHL27 are negative modulators of hypocotyl growth in *Arabidopsis*. *Plant J.* **54,** 1–14
19. Xiao, C., Chen, F., Yu, X., Lin, C., and Fu, Y. F. (2009) Overexpression of an

AT-hook gene, AHL22, delays flowering and inhibits the elongation of the hypocotyl in *Arabidopsis thaliana*. *Plant Mol. Biol.* **71,** 39–50
20. Ng, K. H., Yu, H., and Ito, T. (2009) AGAMOUS controls GIANT KILLER, a multifunctional chromatin modifier in reproductive organ patterning and differentiation. *PLoS Biol.* **7,** e1000251
21. Lu, H., Zou, Y., and Feng, N. (2010) Overexpression of AHL20 negatively regulates defenses in *Arabidopsis*. *J. Integr. Plant Biol.* **52,** 801–808
22. Fujimoto, S., Matsunaga, S., Yonemura, M., Uchiyama, S., Azuma, T., and Fukui, K. (2004) Identification of a novel plant MAR DNA-binding protein localized on chromosomal surfaces. *Plant Mol. Biol.* **56,** 225–239
23. Kim, Y. S., Kim, S. G., Park, J. E., Park, H. Y., Lim, M. H., Chua, N. H., and Park, C. M. (2006) A membrane-bound NAC transcription factor regulates cell division in *Arabidopsis*. *Plant Cell* **18,** 3132–3144
24. Parviz F., Hall D. D., Markwardt D. D., and Heideman W. (1998) Transcriptional regulation of CLN3 expression by glucose in *Saccharomyces cerevisiae*. *J. Bacteriol.* **180,** 4508–4515
25. Yang, S. D., Seo, P. J., Yoon, H. K., and Park, C. M. (2011) The *Arabidopsis* NAC transcription factor VNI2 integrates abscisic acid signals into leaf senescence via the COR/RD genes. *Plant Cell* **23,** 2155–2168
26. Yoo, S. D., Cho, Y. H., and Sheen, J. (2007) *Arabidopsis* mesophyll protoplasts. A versatile cell system for transient gene expression analysis. *Nat. Protoc.* **2,** 1565–1572
27. Hong, S. Y., Kim, O. K., Kim, S. G., Yang, M. S., and Park, C. M. (2011) Nuclear import and DNA binding of the ZHD5 transcription factor is modulated by a competitive peptide inhibitor in *Arabidopsis*. *J. Biol. Chem.* **286,** 1659–1668
28. Takada, S., and Goto, K. (2003) Terminal flower2, an *Arabidopsis* homolog of heterochromatin protein1, counteracts the activation of flowering locus T by constans in the vascular tissues of leaves to regulate flowering time. *Plant Cell* **15,** 2856–2865
29. Schena, M., and Davis, R. W. (1992) HD-Zip proteins, members of an *Arabidopsis* homeodomain protein superfamily. *Proc. Natl. Acad. Sci. U.S.A.* **89,** 3894–3898
30. Sessa, G., Morelli, G., and Ruberti, I. (1993) The Athb-1 and -2 HD-Zip domains homodimerize forming complexes of different DNA binding specificities. *EMBO J.* **12,** 3507–3517
31. Castillejo, C., and Pelaz, S. (2008) The balance between CONSTANS and TEMPRANILLO activities determines FT expression to trigger flowering. *Curr. Biol.* **18,** 1338–1343
32. Santos-Rosa, H., Schneider, R., Bannister, A. J., Sherriff, J., Bernstein, B. E., Emre, N. C., Schreiber, S. L., Mellor, J., and Kouzarides, T. (2002) Active genes are trimethylated at K4 of histone H3. *Nature* **419,** 407–411
33. Litt, M. D., Simpson, M., Gaszner, M., Allis, C. D., and Felsenfeld, G. (2001) Correlation between histone lysine methylation and developmental changes at the chicken β-globin locus. *Science* **293,** 2453–2455
34. Kirmizis, A., Bartley, S. M., Kuzmichev, A., Margueron, R., Reinberg, D., Green, R., and Farnham, P. J. (2004) Silencing of human polycomb target genes is associated with methylation of histone H3K27. *Genes Dev.* **18,** 1592–1605
35. Hollender, C., and Liu, Z. (2008) Histone deacetylase genes in *Arabidopsis* development. *J. Integr. Plant Biol.* **50,** 875–885
36. Vinson, C., Acharya, A., and Taparowsky, E. J. (2006) Deciphering B-ZIP transcription factor interactions *in vitro* and *in vivo*. *Biochim. Biophys. Acta* **1759,** 4–12
37. Jiang, D., Wang, Y., Wang, Y., and He, Y. (2008) Repression of flowering locus C and flowering locus T by the *Arabidopsis* polycomb repressive complex 2 components. *PLoS One* **3,** e3404
38. Turck, F., Roudier, F., Farrona, S., Martin-Magniette, M. L., Guillaume, E., Buisine, N., Gagnot, S., Martienssen, R. A., Coupland, G., and Colot, V. (2007) *Arabidopsis* TFL2/LHP1 specifically associates with genes marked by trimethylation of histone H3 lysine 27. *PLoS Genet.* **3,** e86
39. Silverstein, R. A., Richardson, W., Levin, H., Allshire, R., and Ekwall, K. (2003) A new role for the transcriptional corepressor SIN3. Regulation of centromeres. *Curr. Biol.* **13,** 68–72
40. Metcalf, C. E., and Wassarman, D. A. (2006) DNA binding properties of TAF1 isoforms with two AT-hooks. *J. Biol. Chem.* **281,** 30015–30023